

The temperature dependence of FeRh's transport properties

S. Mankovsky, S. Polesya, K. Chadova and H. Ebert
Department Chemie, Ludwig-Maximilians-Universität München, 81377 München, Germany

J. B. Staunton
Department of Physics, University of Warwick, Coventry, UK

T. Gruenbaum, M. A. W. Schoen and C. H. Back
Department of Physics, Regensburg University, Regensburg, Germany

X. Z. Chen, C. Song
*Key Laboratory of Advanced Materials (MOE), School of Materials
Science and Engineering, Tsinghua University, Beijing 100084, China.*
(Dated: April 3, 2018)

The finite-temperature transport properties of FeRh compounds are investigated by first-principles Density Functional Theory-based calculations. The focus is on the behavior of the longitudinal resistivity with rising temperature, which exhibits an abrupt decrease at the metamagnetic transition point, $T = T_m$ between ferro- and antiferromagnetic phases. A detailed electronic structure investigation for $T \geq 0$ K explains this feature and demonstrates the important role of (i) the difference of the electronic structure at the Fermi level between the two magnetically ordered states and (ii) the different degree of thermally induced magnetic disorder in the vicinity of T_m , giving different contributions to the resistivity. To support these conclusions, we also describe the temperature dependence of the spin-orbit induced anomalous Hall resistivity and Gilbert damping parameter. For the various response quantities considered the impact of thermal lattice vibrations and spin fluctuations on their temperature dependence is investigated in detail. Comparison with corresponding experimental data finds in general a very good agreement.

PACS numbers: Valid PACS appear here

For a long time the ordered equiatomic FeRh alloy has attracted much attention owing to its intriguing temperature dependent magnetic and magnetotransport properties. The crux of these features of this CsCl-structured material is the first order transition from an antiferromagnetic (AFM) to ferromagnetic (FM) state when the temperature is increased above $T_m = 320$ K [1, 2]. In this context the drop of the electrical resistivity that is observed across the metamagnetic transition is of central interest. Furthermore, if the AFM to FM transition is induced by an applied magnetic field, a pronounced magnetoresistance (MR) effect is found experimentally with a measured MR ratio $\sim 50\%$ at room temperature [2–4]. The temperature of the metamagnetic transition as well as the MR ratio can be tuned by addition of small amounts of impurities [2, 5–8]. These properties make FeRh-based materials very attractive for future applications in data storage devices. The origin of the large MR effect in FeRh, however, is still under debate. Suzuki et al. [9] suggest that, for deposited thin FeRh films, the main mechanism stems from the spin-dependent scattering of conducting electrons on localized magnetic moments associated with partially occupied electronic d -states [10] at grain boundaries. Kobayashi et al. [11] have also discussed the MR effect in the bulk ordered FeRh system attributing its origin to the modification of the Fermi surface across the metamagnetic transition. So

far only one theoretical investigation of the MR effect in FeRh has been carried out on an ab-initio level [12].

The present study is based on spin-polarized, electronic structure calculations using the fully relativistic multiple scattering KKR (Korringa-Kohn-Rostoker) Green function method [13–15]. This approach allowed to calculate the transport properties of FeRh at finite temperatures on the basis of the linear response formalism using the Kubo-Středa expression for the conductivity tensor [16, 17]

$$\sigma_{\mu\nu} = \frac{\hbar}{4\pi N\Omega} \text{Trace} \left(\hat{j}_\mu (G^+(E_F) - G^-(E_F)) \hat{j}_\nu G^-(E_F) - \hat{j}_\mu G^+(E_F) \hat{j}_\nu (G^+(E_F) - G^-(E_F)) \right) \chi_c^{-1}$$

where Ω is the volume of the unit cell, N is the number of sites, \hat{j}_μ is the relativistic current operator and $G^\pm(E_F)$ are the electronic retarded and advanced Green functions, respectively, calculated at the Fermi energy E_F . In Eq. (1) the orbital current term has been omitted as it only provides small corrections to the prevailing contribution arising from the first term in the case of a cubic metallic system [18–20].

Here we focus on the finite temperature transport properties of FeRh. In order to take into account electron-phonon and electron-magnon scattering effects in the calculations, the so-called alloy analogy model

[21, 22] is used. Within this approach the temperature induced spin (local moment) and lattice excitations are treated as localized, slowly varying degrees of freedom with temperature dependent amplitudes. Using the adiabatic approximation in the calculations of transport properties, and accounting for the random character of the motions, the evaluation of the thermal average over the spin and lattice excitations in Eq. (1) is reduced to a calculation of the configurational average over the local lattice distortions and magnetic moment orientations, $\langle \dots \rangle_c$, using the recently reported approach [21, 22] which is based on the coherent potential approximation (CPA) alloy theory [23–25].

To account for the effect of spin fluctuations, which we describe in a similar way as is done within the disordered local moment (DLM) theory [26], the angular distribution of thermal spin moment fluctuations is calculated using the results of Monte Carlo (MC) simulations. These are based on ab-initio exchange coupling parameters and reproduce the finite temperature magnetic properties for the AFM and FM state in both the low- ($T < T_m$) and high-temperature ($T > T_m$) regions very well [27]. Figure 1(a), inset, shows the temperature dependent magnetization, $M(T)$, for one of the two Fe sublattices aligned antiparallel/parallel to each other in the AFM/FM state, calculated across the temperature region covering both AFM and FM states of the system. The differing behavior of the magnetic order $M(T)$ in the two phases has important consequences for the transport properties as discussed below.

Figure 1(a) shows the calculated electrical resistivity as a function of temperature, $\rho_{xx}(T)$, accounting for the effects of electron scattering from thermal spin and lattice excitations, and compares it with experimental data. There is clearly a rather good theory-experiment agreement especially concerning the difference $\rho_{xx}^{AFM}(T_m) - \rho_{xx}^{FM}(T_m)$ at the AFM/FM transition, $T_m = 320\text{K}$. The AFM state's resistivity increases more steeply with temperature when compared to that of the FM state, that has also been calculated for temperatures below the metamagnetic transition temperature (dotted line). Note that the experimental measurements have been performed for a sample with 1% intermixing between the Rh and Fe sublattices leading to a finite residual resistivity at $T \rightarrow 0\text{K}$, and as a consequence there is a shift of the experimental $\rho_{xx}(T)$ curve with respect to the theoretical one [28].

We can separate out the contributions of spin fluctuations and lattice vibrations to the electrical resistivities, $\rho_{xx}^{fluc}(T)$ and $\rho_{xx}^{vib}(T)$, respectively. These two components have been calculated for finite temperatures keeping the atomic positions undistorted to find $\rho_{xx}^{fluc}(T)$ and fixed collinear orientations of all magnetic moments to find $\rho_{xx}^{vib}(T)$, respectively. The results for the AFM and FM states are shown in Fig. 1(b), where again the FM (AFM) state has also been considered below (above) the

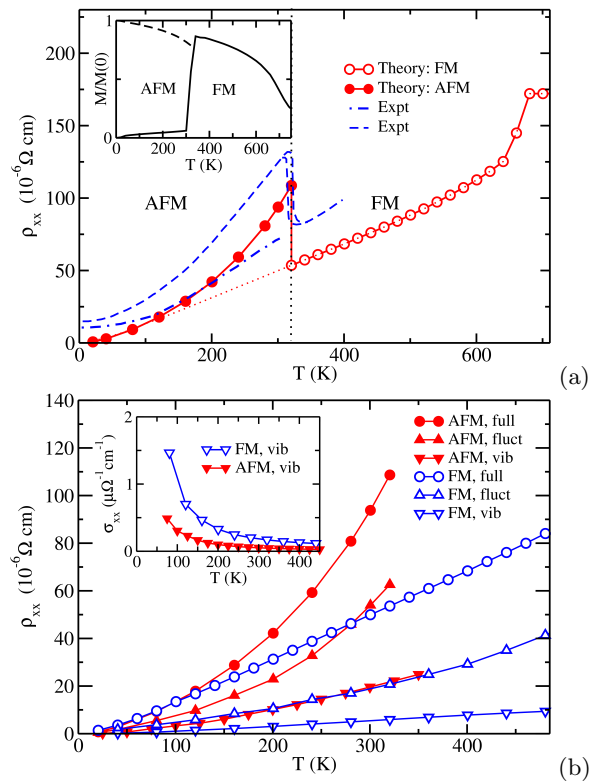


FIG. 1. (a) Calculated longitudinal resistivity (closed circles - AFM state, open circles - FM state) in comparison with experiment [2]. The dashed line represents the results for $\text{Fe}_{0.49}\text{Rh}_{0.51}$, while the dash-dotted line gives results for $(\text{Fe-Ni})_{0.49}\text{Rh}_{0.51}$ with the Ni concentration $x = 0.05$ to stabilize the FM state at low temperature). The inset represents the relative magnetization of a Fe sub-lattice as a function of temperature obtained from MC simulations. (b) electrical resistivity calculated for the AFM (closed symbols) and FM (open symbols) states accounting for all thermal scattering effects (circles) as well as effects of lattice vibrations (diamond) and spin fluctuations (squares) separately. The inset shows the temperature dependent longitudinal conductivity for the AFM and FM states due to lattice vibrations only.

transition temperature T_m . For both magnetic states the local moment fluctuations have a dominant impact on the resistivity. One can also see that both components, $\rho_{xx}^{fluc}(T)$ and $\rho_{xx}^{vib}(T)$, in the AFM state have a steeper increase with temperature than those of the FM state.

The origin of this behavior can be clarified by referring to Mott's model [29] with its distinction between delocalized sp -electrons, which primarily determine the transport properties owing to their high mobility, and the more localized d -electrons. Accordingly, the conductivity should depend essentially on (see. e.g. [30]): (i) the carrier (essentially sp -character) concentration n and (ii) the relaxation time $\tau \sim [V_{scatt}^2 n(E_F)]^{-1}$, where V_{scatt} is the average scattering potential and $n(E_F)$ the total density of states at the Fermi level. This model has been used, in particular, for qualitative discussions of the origin of the GMR effect in heterostructures consisting of

magnetic layers separated by non-magnetic spacers. In this case the GMR effect can be attributed to the spin dependent scattering of conduction electrons which leads to a dependence of the resistivities on the relative orientation of magnetic layers, parallel or antiparallel, assuming the electronic structure of non-magnetic spacer to be unchanged. These arguments, however, cannot be straightforwardly applied to CsCl-structured FeRh, even though it can be pictured as a layered system with one atom thick layers, since the electronic structure of FeRh shows strong modifications across the AFM-FM transition as discussed, for example, by Kobayashi et al. [11] to explain the large MR effect in FeRh.

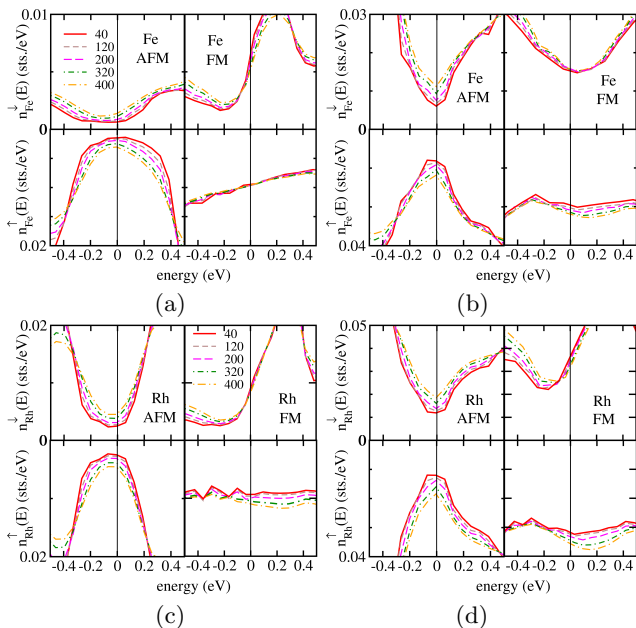


FIG. 2. Comparison of the temperature dependent densities of states (DOS) for the FM and AFM states of FeRh for $T = 40 - 400$ K : (a) Fe s -DOS, (b) Fe p -DOS, (c) Rh s -DOS, and (d) Rh p -DOS.

We use the calculated density of states at the Fermi level as a measure of the concentration of the conducting electrons. The change of the carriers concentration at the AFM-FM transition can therefore be seen from the modification of the sp -DOS at the Fermi level. The element-projected spin-resolved sp -DOS ($n_{sp}(E)$), calculated for both FM and AFM states at different temperatures, is shown in Fig. 2. At low temperature, for both Fe and Rh sublattices, the sp -DOS at E_F is higher in the FM than in the AFM state, $n_{sp}^{FM}(E_F) > n_{sp}^{AFM}(E_F)$. This gives a first hint concerning the origin of the large difference between the FM- and AFM-conductivities in the low temperature limit (see inset for σ_{xx}^{vib} in Fig. 1(b)). In this case the relaxation time τ is still long owing to the low level of both lattice vibrations and spin fluctuations which determines the scattering potential V_{scatt} . For both magnetic states the decrease of the conductiv-

ity with rising temperature is caused by the increase of scattering processes and consequent decrease of the relaxation time. At the same time, the conductivity difference, $\Delta\sigma(T) = \sigma_{xx}^{vib,FM}(T) - \sigma_{xx}^{vib,AFM}(T)$, reduces with increase in temperature. This effect can partially be attributed to the temperature dependent changes of the electronic structure (disorder smearing of the electronic states) reflected by changes in the density of states at the Fermi level [28] (see Fig. 2). Despite this, up to the transition temperature, $T = T_m$, the difference $\Delta\sigma(T)$ is rather pronounced leading to a significant change of the resistivity at $T = T_m$.

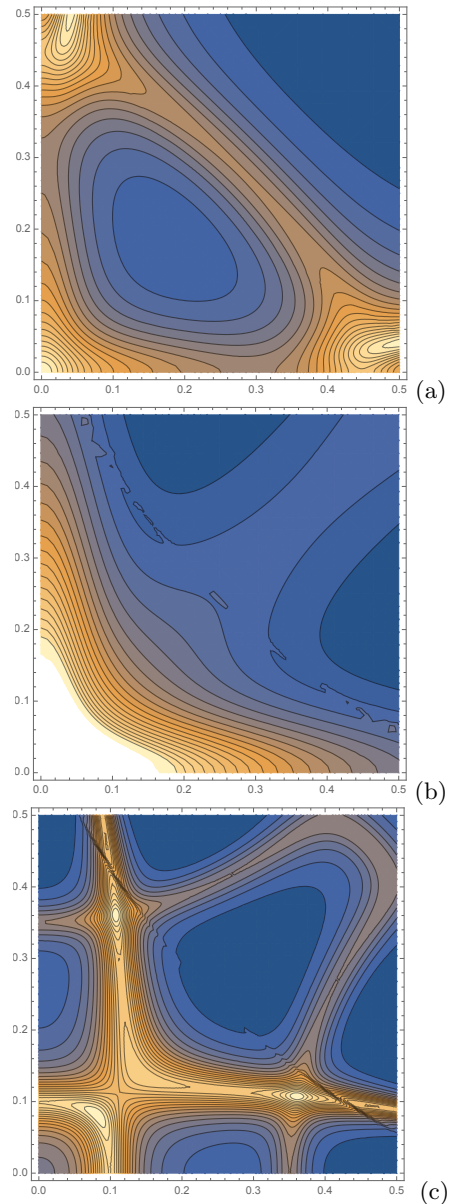


FIG. 3. (a) Bloch spectral function of FeRh calculated for the AFM state at $T = 300$ K (a) and for the FM state resolved into majority spin (b) and minority spin (c) electron components, calculated for $T = 320$ K. The finite width of this features determine the electronic mean free paths.

One has to stress that in calculating the contribution of spin moment fluctuations to the resistivity, the different temperature dependent behavior of the magnetic order in the FM and AFM states must be taken into account. This means, that at the critical point, $T = T_m$, the smaller sublattice magnetization in the AFM state describes a more pronounced magnetic disorder when compared to the FM state which leads to both a smaller relaxation time and shorter mean free path. The result is a higher resistivity in the AFM state.

The different mean free path lengths in the FM and AFM states at a given temperature can be analyzed using the Bloch spectral function (BSF), $A_B(\vec{k}, E)$ [15], calculated for $E = E_F$, since the electronic states at the Fermi level give the contribution to the electrical conductivity. For a system with thermally induced spin fluctuations and lattice displacements the BSF has features with finite width from which the mean free path length of the electrons can be inferred. Fig. 3 shows an intensity contour plot for the BSF of FeRh averaged over local moment configurations appropriate for the FM and AFM states just above and just below the FM-AFM transition respectively. Fig. 3(a) shows the AFM Bloch spectral function whereas Figs. 3(b) and (c) show the sharper features of the spin-polarized BSF of the FM state especially for the minority spin states. This implies a longer electronic mean free path in the FM state in comparison to that in the AFM state which is consistent with the drop in resistivity.

In particular concerning technical applications of FeRh, it is interesting to study further temperature dependent response properties. In Fig. 4(a) we show our calculations of the total anomalous Hall resistivity for FeRh in the FM state, represented by the off-diagonal term ρ_{xy} of the resistivity tensor and compare it with experimental data [11]. As the FM state is unstable in pure FeRh at low temperatures, the measurements were performed for $(\text{Fe}_{0.965}\text{Ni}_{0.035})\text{Rh}$, for which the FM state has been stabilized by Ni doping. The calculations have been performed both, for the pure FeRh compound as well as for FeRh with 5% Ni doping, $(\text{Fe}_{0.95}\text{Ni}_{0.05})\text{Rh}$, which theory finds to be ferromagnetically ordered down to $T = 0$ K. As can be seen the magnitude of $\rho_{xy}(T)$ increases in a more pronounced way for the undoped system. Nevertheless, both results are in a rather good agreement with experiment.

In addition to the temperature dependent transport properties the inclusion of relativistic effects into the ab-initio theory enables us to present results for the Gilbert damping, which plays a crucial role for spin dynamics. We have calculated this quantity taking into account all temperature induced effects, i.e. spin fluctuations and lattice vibrations [32, 33]. As one can see in Fig. 4(b), the calculated results are in rather good agreement with the experimental value (shown by diamond) $\alpha = 0.0012$ obtained for a thick film at $T = 420$ K [31] as well as new ex-

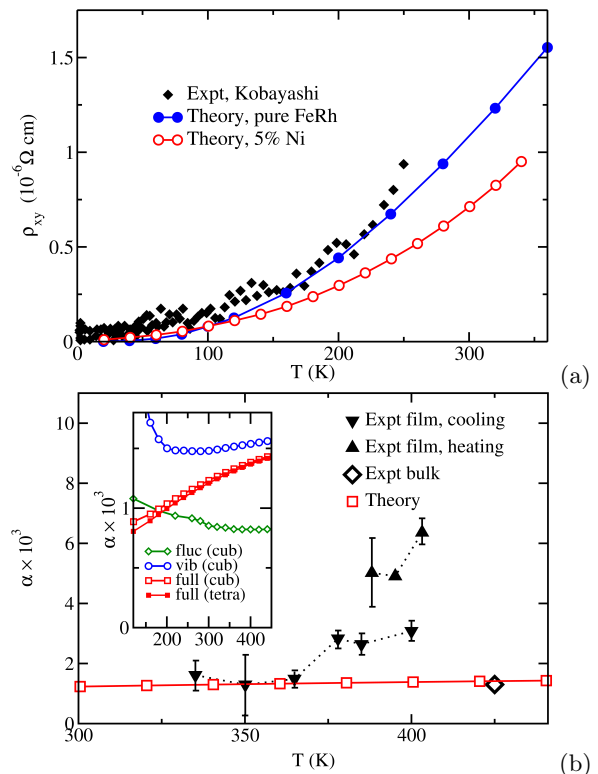


FIG. 4. (a) The temperature dependence of the anomalous Hall resistivity for the FM state of $(\text{Fe}_{0.95}\text{Ni}_{0.05})\text{Rh}$ in comparison with experimental data [11]; (b) Gilbert damping parameter as a function of temperature: theory accounting for all thermal contributions (squares) in comparison with the experimental results for thick-film system (50 nm) [31] (open diamond) and for FeRh thin film deposited on MgO(001) surface (up- and down-triangles). Up- and down-triangles represent data for a heating and cooling cycles, respectively (for details see supplementary materials). The inset represents the results for the individual sources for the Gilbert damping, i.e., lattice vibrations (circles) and spin fluctuations (diamonds). The total α values calculated for FeRh crystal without (c) and with tetragonal (t) distortions ($c/a = 1.016$) are shown by open and closed squares, respectively.

perimental data for thin films [15]. The separate contributions to the Gilbert damping due to spin fluctuations and lattice vibrations are presented in the inset to Fig. 4(b) for a given temperature window again artificially extended to low temperatures. These results allow to identify the leading role of lattice vibrations (circles in the inset to Fig. 4(b)) at high temperature region where the electron spin-flip interband transitions are most responsible for dissipation due to the magnetization dynamics. In the low-temperature region, where the T -dependence of α is determined by intraband spin-conserving scattering events, it stems dominantly from electron scattering due to thermally induced spin-fluctuations (diamonds in the inset to Fig. 4(b)).

The experimental data shown in Fig. 4(b) by triangles represent results for rather thin films ($d = 25$ nm)

deposited on top of a MgO(001) substrate [15]. The FeRh unit cell with a lattice constant $\sqrt{2}$ times smaller than that of MgO, is rotated around z axis by 45° with respect to the MgO cell. Because of this, a compressive strain in the FeRh film occurs. As it follows from the experimental data [34], this implies a tetragonal distortion of the FM FeRh unit cell with $c/a = 1.016$. Results of corresponding calculations for α are given in the inset of Fig. 4(b) by full squares, demonstrating a rather weak effect of this distortion. The smaller value of α compared to experiment, has therefore to be attributed to the use of bulk geometry instead of the experimental film geometry with a corresponding impact on the damping parameter.

In summary, we have presented ab-initio calculations for the finite temperature transport properties of the FeRh compound. A steep increase of the electric resistivity has been obtained for the AFM state leading to a pronounced drop of resistivity at the AFM to FM transition temperature. This effect can be attributed partially to the difference of the electronic structure of FeRh in the FM and AFM states, as well as to a faster increase of the amplitude of spin fluctuations caused by temperature in the AFM state. Further calculated temperature dependent response properties such as the AHE resistivity and the Gilbert damping parameter for the FM system show also good agreement with experimental data. This gives additional confidence in the model used to account for thermal lattice vibrations and spin fluctuations.

ACKNOWLEDGEMENTS

Financial support by the DFG via SFB 689 (Spinphänomene in reduzierten Dimensionen) and from the EPSRC (UK) (Grant No. EP/J006750/1) is gratefully acknowledged.

-
- [1] J. S. Kouvel and C. C. Hartelius, *J. Appl. Phys.* **33** (1962).
- [2] N. Baranov and E. Barabanova, *Journal of Alloys and Compounds* **219**, 139 (1995), eleventh international conference on solid compounds of transition elements.
- [3] P. A. Algarabel, M. R. Ibarra, C. Marquina, A. del Moral, J. Galibert, M. Iqbal, and S. Askenazy, *Applied Physics Letters* **66**, 3061 (1995).
- [4] M. A. de Vries, M. Loving, A. P. Mihai, L. H. Lewis, D. Heiman, and C. H. Marrows, *New Journal of Physics* **15**, 013008 (2013).
- [5] P. H. L. Walter, *Journal of Applied Physics* **35**, 938 (1964).
- [6] J. S. Kouvel, *Journal of Applied Physics* **37**, 1257 (1966).
- [7] R. Barua, F. Jimnez-Villacorta, and L. H. Lewis, *Applied Physics Letters* **103**, 102407 (2013).
- [8] W. Lu, N. T. Nam, and T. Suzuki, *Journal of Applied Physics* **105**, 07A904 (2009).
- [9] I. Suzuki, T. Naito, M. Itoh, T. Sato, and T. Taniyama, *Journal of Applied Physics* **109**, 07C717 (2011).
- [10] M. Knülle, D. Ahlers, and G. Schütz, *Solid State Commun.* **94**, 267 (1995).
- [11] Y. Kobayashi, K. Muta, and K. Asai, *Journal of Physics: Condensed Matter* **13**, 3335 (2001).
- [12] J. Kudrnovský, V. Drchal, and I. Turek, *Phys. Rev. B* **91**, 014435 (2015).
- [13] H. Ebert et al., *The Munich SPR-KKR package*, version 6.3, H. Ebert et al. <http://olymp.cup.uni-muenchen.de/ak/ebert/SPRKKR> (2012).
- [14] H. Ebert, D. Ködderitzsch, and J. Minár, *Rep. Prog. Phys.* **74**, 096501 (2011).
- [15] see supplementary materials, .
- [16] P. Středa, *J. Phys. C: Solid State Phys.* **15**, L717 (1982).
- [17] S. Lowitzer, D. Ködderitzsch, and H. Ebert, *Phys. Rev. B* **82**, 140402(R) (2010).
- [18] T. Naito, D. S. Hirashima, and H. Kontani, *Phys. Rev. B* **81**, 195111 (2010).
- [19] S. Lowitzer, M. Gradhand, D. Ködderitzsch, D. V. Fedorov, I. Mertig, and H. Ebert, *Phys. Rev. Lett.* **106**, 056601 (2011).
- [20] I. Turek, J. Kudrnovský, and V. Drchal, *Phys. Rev. B* **86**, 014405 (2012).
- [21] H. Ebert, S. Mankovsky, D. Ködderitzsch, and P. J. Kelly, *Phys. Rev. Lett.* **107**, 066603 (2011), <http://arxiv.org/abs/1102.4551v1>.
- [22] H. Ebert, S. Mankovsky, K. Chadova, S. Polesya, J. Minár, and D. Ködderitzsch, *Phys. Rev. B* **91**, 165132 (2015).
- [23] B. Velický, *Phys. Rev.* **184**, 614 (1969).
- [24] W. H. Butler, *Phys. Rev. B* **31**, 3260 (1985).
- [25] I. Turek, J. Kudrnovský, V. Drchal, L. Szunyogh, and P. Weinberger, *Phys. Rev. B* **65**, 125101 (2002).
- [26] B. L. Gyorffy, A. J. Pindor, J. Staunton, G. M. Stocks, and H. Winter, *J. Phys. F: Met. Phys.* **15**, 1337 (1985).
- [27] S. Polesya, S. Mankovsky, D. Ködderitzsch, J. Minár, and H. Ebert, *Phys. Rev. B* **93**, 024423 (2016).
- [28] J. B. Staunton, M. Banerjee, dos Santos Dias, A. Deak, and L. Szunyogh, *Phys. Rev. B* **89**, 054427 (2014).
- [29] N. F. Mott, *Adv. Phys.* **13**, 325 (1964).
- [30] E. Y. Tsymbal, D. G. Pettifor, and S. Maekawa, “Giant magnetoresistance: Theory,” in *Handbook of Spin Transport and Magnetism*, edited by E. Y. Tsymbal and I. Zutic (Taylor and Francis Group, New York, 2012).
- [31] E. Mancini, F. Pressacco, M. Haertinger, E. E. Fullerton, T. Suzuki, G. Woltersdorf, and C. H. Back, *Journal of Physics D: Applied Physics* **46**, 245302 (2013).
- [32] S. Mankovsky, D. Ködderitzsch, G. Woltersdorf, and H. Ebert, *Phys. Rev. B* **87**, 014430 (2013).
- [33] H. Ebert, S. Mankovsky, K. Chadova, S. Polesya, J. Minár, and D. Ködderitzsch, *Phys. Rev. B* **91**, 165132 (2015).
- [34] C. Bordel, J. Juraszek, D. W. Cooke, C. Baldasseroni, S. Mankovsky, J. Minár, H. Ebert, S. Moyerman, E. E. Fullerton, and F. Hellman, *Phys. Rev. Lett.* **109**, 117201 (2012).